

Gram-Scale Synthesis of 1,8-Naphthyridines in Water: The Friedlander Reaction Revisited

Shubhranshu Shekhar Choudhury, Subhrakant Jena, Dipak Kumar Sahoo, Shamasoddin Shekh, Rajiv K. Kar, Ambuj Dhakad, Konkallu Hanumae Gowd, and Himansu S. Biswal*



Cite This: *ACS Omega* 2021, 6, 19304–19313



Read Online

ACCESS |



Metrics & More

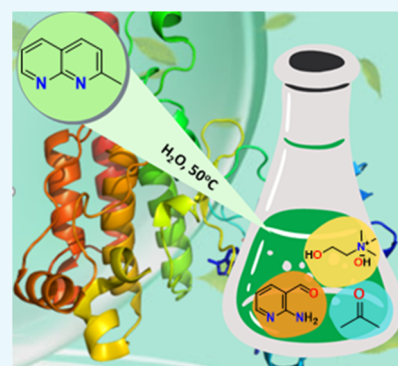


Article Recommendations



Supporting Information

ABSTRACT: The products of the Friedlander reaction, i.e., 1,8-naphthyridines, have far-reaching impacts in materials science, chemical biology, and medicine. The reported synthetic methodologies elegantly orchestrate the diverse synthetic routes of naphthyridines but require harsh reaction conditions, organic solvents, and expensive metal catalysts. Here, we introduce gram-scale synthesis of 1,8-naphthyridines in water using an inexpensive and biocompatible ionic liquid (IL) as a catalyst. This is the first-ever report on the synthesis of naphthyridines in water. This is a one-step reaction, and the product separation is relatively easy. The choline hydroxide (ChOH) is used as a metal-free, nontoxic, and water-soluble catalyst. In comparison to other catalysts reported in the literature, ChOH has the advantage of forming an additional hydrogen bond with the reactants, which is the vital step for the reaction to happen in water. Density functional theory (DFT) and noncovalent interaction (NCI) plot index analysis provide the plausible reaction mechanism for the catalytic cycle and confirm that hydrogen bonds with the IL catalyst are pivotal to facilitate the reaction. Molecular docking and molecular dynamics (MD) simulations are also performed to demonstrate the potentialities of the newly synthesized products as drugs. Through MD simulations, it was established that the tetrahydropyrido derivative of naphthyridine (**10j**) binds to the active sites of the ts3 human serotonin transporter (hSERT) (PDB ID: 6AWO) without perturbing the secondary structure, suggesting that **10j** can be a potential preclinical drug candidate for hSERT inhibition and depression treatment.



INTRODUCTION

The medicinal properties of naphthyridines and their derivatives are the major driving forces to synthesize them on a large scale. Among naphthyridines, 1,8-naphthyridines (**1**, Figure 1A) and their derivatives are used as drugs for antimicrobial activities (nalidixic acid, **2**),^{1–4} HIV inhibitor (**3**),⁵ antibacterial activities (gemifloxacin, **4**),^{6,7} antitumor activity (vosaroxin, **5**), etc.^{8–10} The 1,8-naphthyridine derivatives can also act as monodentate, bidentate, or binucleating bridging ligands (**6**, Figure 1A).^{11–15} They also exhibit excellent thermally activated delayed fluorescence (TADF) and high photoluminescence quantum yield (**7**),¹⁶ which make them suitable blue organic light-emitting diodes (OLEDs). It is worth mentioning that the extensively substituted 1,8-naphthyridines and less substituted ones are used as probes to monitor the structure and function of enzymes and proteins. For example, 1,8-naphthyridine-2-carboxylic acid acts as a doorstop for co-factor entry in FAD/NAD-linked reductase (Figure 1B).¹⁷ Similarly, 4-bromo-1,8-naphthyridine is used as a FragLite to identify ligand-binding sites in proteins.¹⁸ However, sustainable and scalable synthesis of these drug-like molecules remains challenging ever since Friedlander introduced the synthesis of naphthyridine by condensing o-aminobenzaldehyde with

acetaldehyde in the presence of sodium hydroxide¹⁹ in 1882 (Friedlander reaction). In 1927, Koller's group reported the synthesis of 1,8-naphthyridines for the first time.²⁰ The improved Friedlander reactions use various catalysts, and organic solvents such as ligand-free copper catalyst in dimethylformamide (DMF),²¹ ruthenium nanolayer in mesitylene,²² Hf-UiO-66-N₂H₃ metal–organic framework catalyst,²³ trifluoroacetic acid in DMSO,²⁴ and some recent advances can be found elsewhere.²⁵ The studied catalysts and solvents used for the Friedlander reaction exhibit high cost, toxicity, high loading, low selectivity, high-temperature dependence, etc., which contribute to environmental pollution, limiting the criteria for green synthesis.^{26,27} Thus, sustainable approaches need to be explored from a green perspective point of view, and a recent review sheds light on the greener synthesis of quinolone that uses water as the solvent.²⁸ It is advantageous to choose water as a solvent in the reaction

Received: May 28, 2021

Accepted: June 29, 2021

Published: July 12, 2021



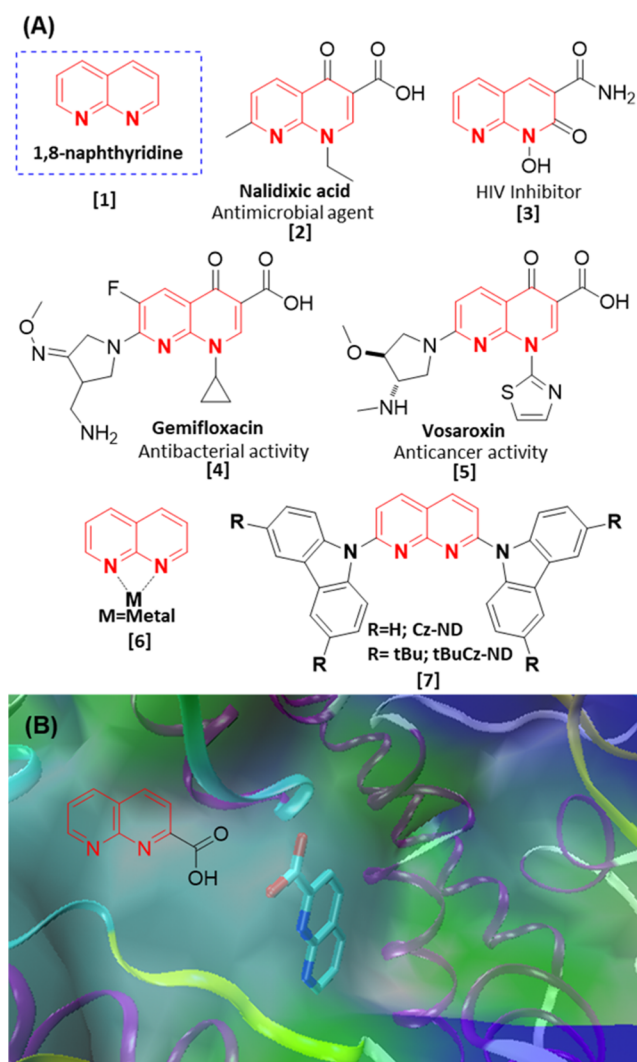
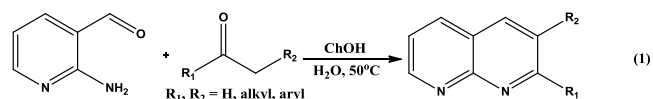


Figure 1. (A) Examples of 1,8-naphthyridine derivatives used as drugs, chelating ligands, and organic light-emitting diodes (OLEDs). (B) 1,8-Naphthyridine derivatives used as doorstop for co-factor entry in FAD/NAD-linked reductase (PDB ID: 6FP4).

medium.²⁹ Very recently, Hayes and co-workers reported the synthesis of 1,8-naphthyridine and its derivatives in moderate to good yield^{30,31} using metal hydroxides (LiOH and KOH) in aqueous-alcohol media. Although there are a few reports on the synthesis of quinoline derivatives using the Friedlander reaction in mixed aqueous-alcohol media, using metal-based catalysts such as Fe_3O_4 -IL- HSO_4 ,³¹ $\text{LiOH}\cdot\text{H}_2\text{O}$ ³⁰ makes them unfavorable from the green chemistry perspective. The quest for developing eco-friendly synthetic methods using greener routes has remained challenging since the last century. This approach includes the utility of aqueous solvent, metal-free catalysts, and nontoxic byproducts without compromising reaction yield. Over the years, many organic compounds have been successfully synthesized, considering this sustainable approach.^{32–34} Denis Prat et al. reported their survey, which guides in selecting a solvent³⁵ for a chemical reaction. Water has several desirable properties such as cost-effectiveness, safety, abundance, and environmentally benign nature, ensuring an alternative solvent. However, solubility limitations of reactants are deterrents to water as the reaction medium.³⁶ Fortunately, most of the reactants of the Friedlander

condensation reaction are soluble in water. Hence, this work aims to carry out the gram-scale synthesis of 1,8-naphthyridine derivatives through Friedlander condensation in water without using metal hydroxides or metal catalysts. Ionic liquids have emerged as a green substitute to many other organic solvents and catalysts in the field of catalysis.^{37–39} As an alternative, choline hydroxide (ChOH) is used as a metal-free, nontoxic, and water-soluble catalyst to synthesize 1,8-naphthyridine derivatives under conditions to avoid hazardous or carcinogenic organic solvents.^{40,41} This is in line with our continuous effort to explore and prove that choline-based ionic liquids (ILs) are alternative avenues for synthesis, enzymatic activity, drug solubility, and, most importantly, storage and stability of DNA and proteins.^{42–44}

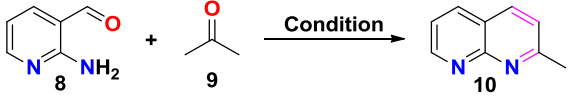


In this work, we chose 2-aminonicotinaldehyde (8) as a key starting material that possesses one *N*-containing ring (pyridine) that reacts with the active methylene carbonyl groups to form another pyridine ring through Friedlander condensation (eq 1). The products were obtained in excellent yield. Further, ChOH-IL was successfully separated from the reaction mixture without using any chromatographic methodology. The plausible reaction mechanism using quantum chemical calculations was proposed for the first time. Thus, our objective is threefold: (a) to propose an alternative synthesis method for the gram-scale synthesis of 1,8-naphthyridine and its derivatives in water, (b) the role of hydrogen bonding by the ChOH-IL (catalyst) for high product yield through in-depth quantum chemical calculation, and (c) possible use of the newly synthesized products as potential drugs. In this work, we highlight (i) a combinatorial approach of synthesis, (ii) DFT and noncovalent interaction (NCI) analysis, and (iii) biophysical analysis through toxicity prediction and MD simulations, to bring to notice that the choice of ChOH IL-based metal-free aqueous catalysis has multitude benefits over other expensive and toxic catalysts that enabled us to carry out Friedlander reaction in a sustainable way with gram-scale product yield.

RESULTS AND DISCUSSION

Gram-Scale Synthesis in Water. We started the synthesis by choosing 2-aminonicotinaldehyde (8) and acetone (9, with active α -methyl carbonyl group) as the model substrates. With varying molar ratios of ChOH/ H_2O , we optimized the reaction yield at water bath temperature (50 °C) and room temperature (rt) under N_2 atmosphere. The results are presented in Table 1.

The condensation reaction proceeds on stirring the reaction mixture for ~6 h. When the reaction was performed in the absence of the catalyst (ChOH) and solvent (water) under the same condition, we did not observe any product formation (entry 1). Further, no product was formed (entry 2) when water was used as the solvent without catalyst. We also tried this reaction using excess acetone both as reactant and solvent (entry 3) in the absence of the catalyst. However, it also ended up with no product formation. Finally, the desired product 10 was obtained when an excess of acetone was used in the presence of the catalyst, but the yield was less (entry 4, 52% yield). Surprisingly, the desired product was formed with 99% yield (entry 5) at 50 °C when water was used as the solvent

Table 1. Optimization of the Synthesis of 2-Methyl-1,8-naphthyridine^{ab} (10)


entry	cat. (mol %)	solvent	temp. (°C)	time (h)	yield (%)
1			50	10	NR
2		H ₂ O	50	12	NR
3		acetone	50	10	NR
4	ChOH(1)	acetone	50	24	52
5	ChOH(1)	H ₂ O	50	6	99
6	ChOH (1)	H ₂ O	rt	22	90
7	ChOH (0.5)	H ₂ O	50	12	95
8	ChOH (0.5)	H ₂ O	rt	24	57
9	NaOH	H ₂ O	50	6	88
10	KOH	H ₂ O	50	6	84
11	Et ₃ N	H ₂ O	50	6	NR
12	Et ₃ N·(CH ₂ OH) ₂ ^c	H ₂ O	50	6	NR

^aReaction condition: 2-aminonicotinaldehyde, **8** (0.5 mmol), and acetone, **9** (0.5 mmol) were stirred with ChOH (1 mol %) in H₂O (1 mL). ^bIsolated yield, rt: room temperature NR: no reaction. ^c1:1 mixture.

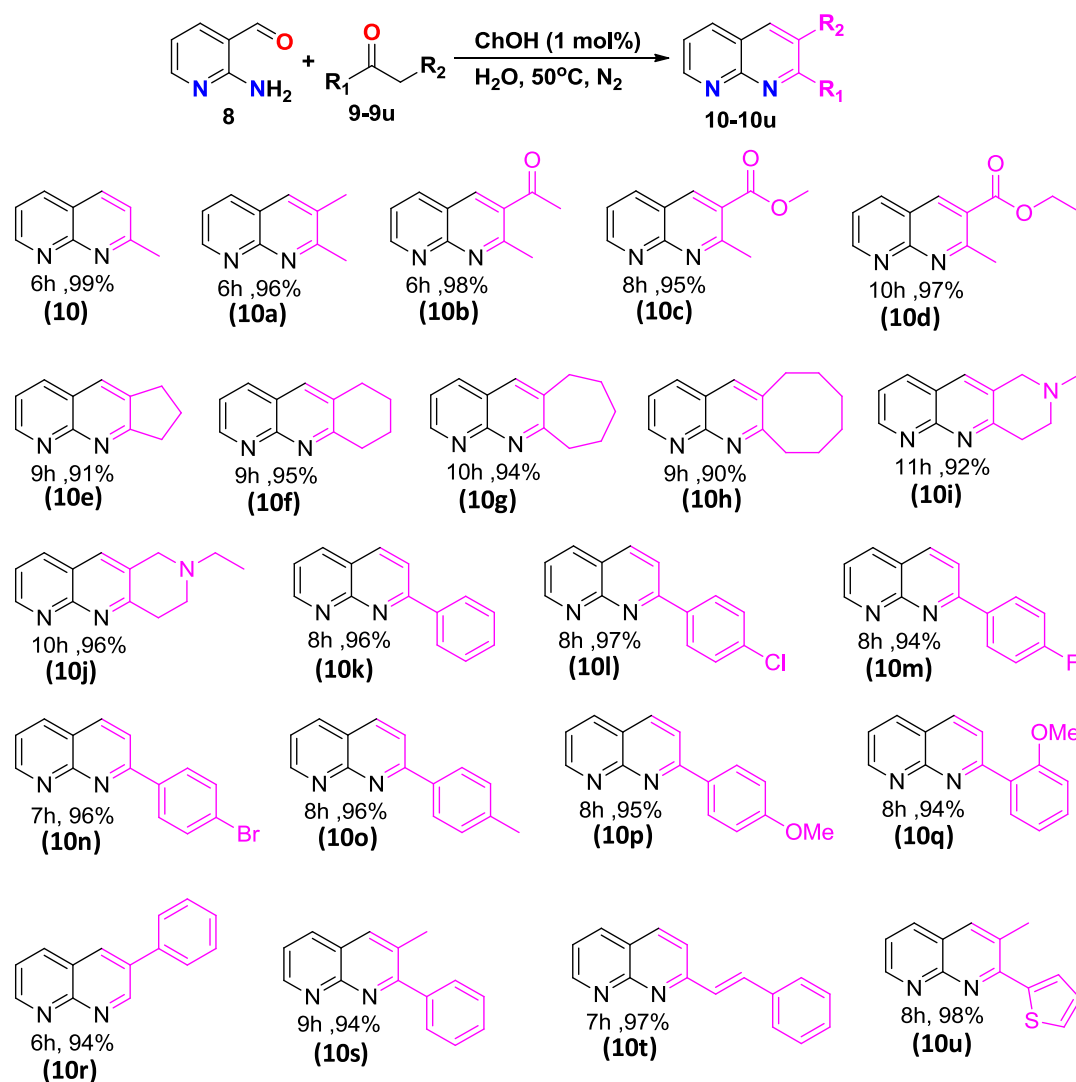
and ChOH as the catalyst. The same reaction was also performed at room temperature, for which the yield was found to be comparatively less (**entry 6, 90% yield**), and apparently, it took longer time to attain equilibrium, which, however, lies mainly in favor of the product formation. We optimized the catalyst mole percent and observed that 1 mol% ChOH gave the optimum yield at room temperature and 50 °C (**entries 5–8**). The virtual completion of all of the reactions was monitored by thin-layer chromatography (TLC), followed by NMR spectroscopy and mass spectrometry characterization. The optimized synthetic procedure highlights the importance of both catalyst (ChOH) and solvent (H₂O) in the reaction medium to obtain an excellent yield of 2-methyl-1,8-naphthyridine (**entry 5**). We also performed the same reaction by considering a few regularly used bases as catalysts (**entry 9–12**), and in all of the cases, the ChOH catalyst was found to be superior to others. After developing a suitable reaction condition, we explored the various substrate scopes of the Friedlander reaction using different active methylene carbonyl groups (**Scheme 1**). Both aromatic and aliphatic (cyclic and acyclic) active methylene carbonyls were considered. To our delight, we obtained all desired products of substituted 1,8-naphthyridines with excellent yield (>90% yield). The products **10–10d** were synthesized from acyclic aliphatic carbonyls with more than 95% yield. It is worth mentioning that Hayes and co-workers synthesized **10b** with 69% yield using LiOH·H₂O in the aqueous medium.³⁰ But in comparison, our synthetic methodology turned out superior (98% product yield) and more efficient for the synthesis of **10b**, which can be used as a precursor of many biologically important compounds. By taking N-heterocyclic active methylene carbonyl substrates, we synthesized two new products, **10i** and **10j**, with excellent yields with additional N-site that needs to be exploited for metal binding^{45,46} in template-assisted ligand reaction.^{47,48} Entries **10e–j** in **Scheme 1** were obtained from aliphatic cyclic carbonyl substrates with excellent yields. These cyclic aliphatic carbonyl products have importance in biology as well as in medicinal chemistry.^{49–51}

The product **10h** moiety possessed inhibitor activity.⁵² Excellent yields were also obtained from aromatic active methylene carbonyl substrates. Notably, the amount of catalyst used is minimal in this reaction, and conversion is more than 90% for all of the substrates. Further, a similar reaction was also carried out on a large scale. The mixture of 2-aminonicotinaldehyde, **8** (1.23 g, 10 mmol), and acetone, **9** (740 μL, 10 mmol) was stirred in H₂O (10 mL) followed by the addition of ChOH (3 μL, 1 mol %). The desired product **10** was obtained with a 92% yield (**1.32 gm**) and confirmed through mass and NMR characterization. Further, we tried to synthesize **10i** and **10j** in gram scale with the same catalyst amount (1 mol %) and the same reaction condition; the products were obtained with 90% (**1.80 gm**) and 95% (**2.04 gm**) yields, respectively. However, when **8** reacted with cyclooctanone under the same reaction conditions with the same catalyst (1 mol %), only a trace amount of product formation was observed. After that, we increased the catalyst amount to 2 mol % under the same reaction conditions; then, product **10h** was formed with 88% (**1.871 gm**) yield. The NMR characterization details for all of the substrates shown in **Scheme 1** are provided in the Supporting Information (**Figures S1–S22**).

Plausible Reaction Mechanism and the Role of Hydrogen Bonding for High Product Yield. Hydrogen-bond (H-bond)-mediated catalysis has proven to be an essential paradigm in facilitating many organic reactions.^{25,53–56} To gain insight into the plausible reaction mechanism and the importance of H-bonds with ChOH, density functional theory (DFT) calculations were performed. Energetics of intermediates and transition states were calculated to construct the reaction pathway that leads to the formation of **10**. The proposed mechanism is given in **Figure 2**. The ChOH acts as a proton acceptor and hydrogen-bond donor. As shown in **Figure 2**, the initiation of the reaction proceeds through activation of the carbonyl group of **9** by the hydroxyl group of choline cation through H-bond, and at the same time, the hydroxide anion of ChOH interacts with α-hydrogen of methylene carbonyl (**INT-1**). The active α-hydrogen was abstracted by hydroxide anion and formed nucleophilic intermediate (**INT-2**) via transition state (**TS-1**) with a barrier energy of 3 kcal mol⁻¹. This smaller reaction barrier is because of the stabilization of **TS-1** through H-bonds.

Further noncovalent interaction (NCI) analysis^{57,58} was performed on the transition states to delineate the importance of H-bonds for transition-state stabilization and low reaction barrier. The NCI plots are helpful to distinguish the strong and weak interactions.^{59–61} The NCI plots for the transition states are shown in **Figure 2** (bottom). The blue-colored isosurface between the OH group of Ch cation and C=O of the reaction indicates strong O-H...O=C H bond in the **TS-1**. Then, the active **INT-2** attacks the carbonyl carbon of **8** to form a stable intermediate, **INT-3**, through the transition state, **TS-2**, with an activation energy barrier of 25.7 kcal mol⁻¹ with respect to **INT-2**. **TS-2** shows the importance of water in the reaction medium. Here, water simultaneously interacts with the anionic carbon of the active methylene group and the O-atom of carbonyl through H-bonds (though weak interactions), whereas the OH group of Ch cation forms a strong H-bond with the C=O of **8**.

It seems this step is the rate-limiting step with the highest activation energy. The hydroxide anion of ChOH interacts with the NH₂ group of **INT-3**, which accelerates to form a six-

Scheme 1. Substrate Scopes of Various Active Methylene Carbonyls for the Synthesis of Substituted 1,8-Naphthyridines^{ab}

^aReaction conditions: **8** (0.5 mmol), **9–9u** (0.5 mmol), ChOH (1 mol %) in H₂O (1 mL). ^bIsolated yield.

membered cyclic structure via intramolecular reaction. The subsequent step yields INT-4 as the lone pair over N, which attacks the C of the carbonyl group via TS-3 by crossing a high energy barrier of 20.6 kcal mol⁻¹. The magnitudes of these activation energy barriers are much less than those reported for the synthesis of tetrasubstituted imidazole [2-(2,4,5-triphenyl-1 H-imidazol-1-in the presence of ethanolamine in [Et₂NH₂][HSO₄]] ionic liquid (IL) as a catalyst,⁶² suggesting that ChOH-ILs are better catalysts for such condensation reactions; the additional H-bond donor group in ChOH is responsible for better catalytic efficiency. During this intramolecular cyclization process, a proton was abstracted by hydroxide anion from the quaternary N-atom of the amine group in TS-3 and released a water molecule. The reaction was followed by abstraction of NH proton and formed an imine bond via intramolecular reaction with release of a water molecule in TS-4 and resulted in INT-5. After that, INT-5 was stabilized by H-bonds with ChOH. INT-5 resulted in the desired product **10** by overcoming a lower energy barrier. In TS-5, the hydroxyl group of choline donates a proton to the O atom, which accelerates to remove water and simultaneously forms a new heterocyclic aromatic ring with the release of -23.1 kcal mol⁻¹

of free energy. The energy barrier for the transition states TS-4 and 5 were surprisingly found to be 1.8 and 1.1 kcal mol⁻¹, respectively. Such reduced activation energy barrier compared to those of previous steps can be attributed to the ring aromatization. Due to the favorable energetic pathway, the desired product **10** was formed quickly, and ChOH was recovered for further use. It seems a little bit of heating is required to overcome the reaction barriers in the initial steps of the reaction. Throughout the reaction, steps such as protonation, deprotonation, and release of water molecules were facilitated by H-bonds between the reactants, intermediates, catalyst (ChOH), and the solvent, H₂O. Hence the importance of H-bonds and the role of H-bond forming catalyst ChOH should carefully be considered for higher product yield.

■ PRODUCTS AS POTENTIAL DRUG CANDIDATES

Assessment for Drug-Likeness. We computed ADMET (absorption, distribution, metabolism, elimination, and toxicity)^{63–66} of all of the 22 substituted 1,8-naphthyridine molecules synthesized to analyze their suitability as potential drug candidates. Lipinski's "Rule of Five" (r05)⁶⁷ was used to

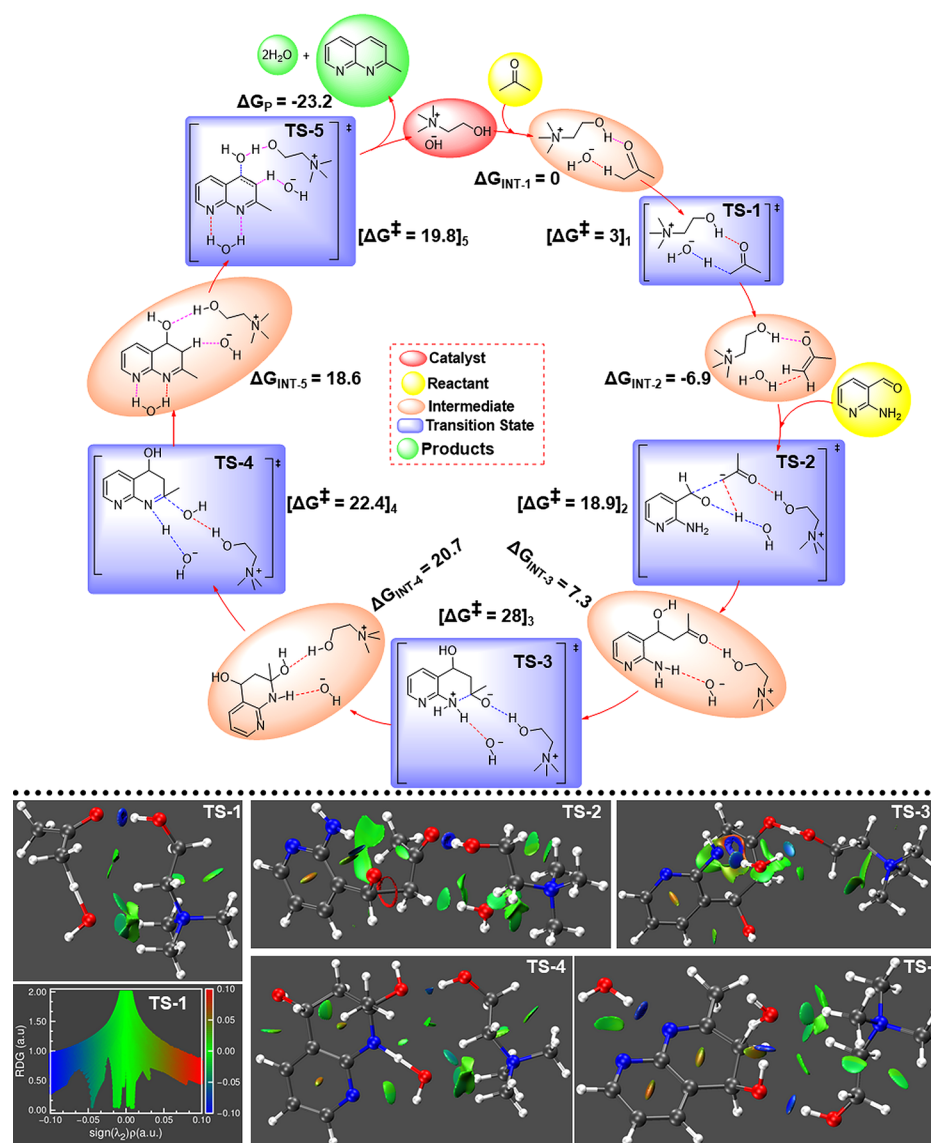


Figure 2. Top: Catalytic cycle designed for the Friedlander reaction involving interaction with one ChOH-IL ion pair to see the IL catalytic and H-bond effects in the solution (H_2O as solvent) at 1 atm and 323 K. Gibbs free energies and enthalpies were calculated relative to reactants (**8**, **9**) + ChOH. The geometry optimization and frequency calculations were performed at the B3LYP-PCM/6-31 + G(d,p) level of theory using the PCM solvation model. Single-point electronic energies were taken from the calculation performed at the B3LYP-PCM/6-311 ++ G(d,p) level of theory. **Bottom:** NCI plot and density gradient plot to show the H-bonds involving the catalyst ChOH-IL. Gradient isosurface follows a blue-green, red color scheme over the range of $-0.04 < \text{sign}(\lambda_2)\rho < +0.04$, where blue, green, and red colors denote very strong attraction, weak interaction, and strong repulsion, respectively.

test the "drug-likeness" quality of the designed drugs. The properties or descriptors that were considered for r05 along with their range were as follows: molecular weight (MW) < 500, lipophilicity ($Q_{p=}$ $\log P_o/w < 5$), hydrogen-bond donors ($HB_{\text{donor}} \leq 5$), hydrogen-bond acceptors ($HB_{\text{accept}} \leq 10$). As presented in Table S1, all of the substituted 1,8-naphthyridine drugs aimed at pharmacological applications showed excellent drug-likeness properties without violating Lipinski's ro5. Hence, these molecules might be helpful in pharmaceutical applications.

Bioavailability Prediction. Jorgensen implemented the "rule of three" (ro3) to predict the bioavailability of drug molecules. If any compound follows some or all of the rules ($Q\text{PlogS} > -5.7$, $Q\text{PPCaco} > 22$ nm/s and # metab < 7) as presented in Table S2, then it is considered to be orally viable.⁶⁸ The bioavailability of any compound is dependent on

the absorption and liver first-pass metabolism processes.⁶⁴ The absorption process, on the other hand, depends on the permeability, solubility, and interactions of the compound with gut wall metabolizing action and transporter enzymes. The computed QikProp values predicted by Jorgensen's r03 are within the limit, which indicates that all naphthyridine-substituted molecules satisfy the bioavailability property to be used as potential drugs.

The 12 most essential and relevant molecular descriptors computed by QikProp are used to calculate the #star parameters (Schrödinger 2011d). These are useful in selecting and optimizing the possibility of using naphthyridine-substituted molecules as drug molecules. These selected #star parameters are as follows: number of rotatable bonds (#rotor: 0–15), total solvent-accessible surface area with 1.4 Å probe radius (SASA: 300–1000 Å²), the hydrophobic

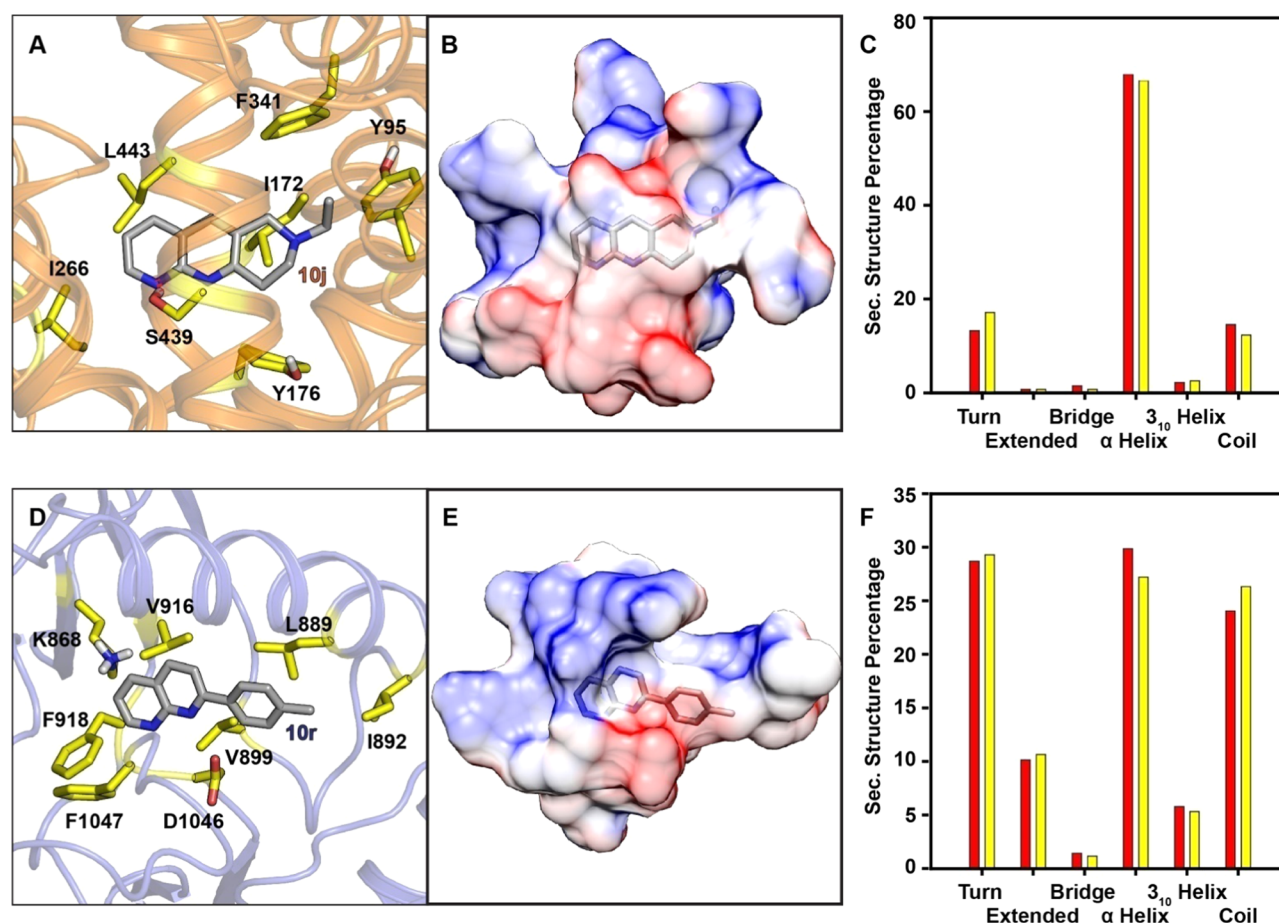


Figure 3. Snapshot from MD simulation trajectory showing the interaction of (A) molecule 10j with human serotonin transporter (HST) (PDB ID: 6AWO) and (D) molecule 10r with VEGFR-2 (PDB ID: 3EFL), within the binding site. Residue numbering was obtained from the PDB files 6AWO and 3EFL, which are used to model the protein environment. Active-site surface representation (residues within 5 Å of the molecule) with the color scheme according to their electrostatic potential is shown for (B) 10j-6AWO and (E) 10r-3EFL. Histogram showing the percentage of secondary structural content based on MD trajectories of (C) 6AWO in red and 10j complexed with 6AWO in yellow and (F) 3EFL in red and 10r complexed with 3EFL in yellow.

component of the solvent-accessible surface area (FOSA: 0–750 Å²), the total solvent-accessible volume of the molecule (probe radius: 1.4 Å, volume: 500–2000 Å³), index of cohesive interaction in solids (ACxDNA.5/SA: 0.0–0.05), globularity descriptor (glob: 0.75 to 0.95), predicted polarizability (QPpolr: 13.0–70.0 for 95% of drugs), predicted IC₅₀ value for blockage of HERG K⁺ channels (QPlogHERG, < -5), logarithm of predicted blood/brain partition coefficient (QPlogBB: -3.0–1.0), predicted apparent MDCK cell permeability in nm/s (QPPMDCK: < 25 poor, > 500 great), predicted skin permeability (QPlogKp: -8.0 to -1.0), logarithm of predicted binding constant to human serum albumin (QPlogKhsa: -1.5 to 1.2). It was found that all of the naphthyridines synthesized in this work exhibited potential drug properties, as shown in Table S3.

10j and 10r as Potential Inhibitors for Human Serotonin Transporter (hSERT) and Protein Kinases Revealed from MD Simulation. ADMET analysis indicates molecules 10–10u being potential drug candidates. In line with this, further investigation of their biophysical properties, such as binding free energies, binding residues, and binding orientations, was conducted through molecular dynamics simulations. Here, we considered hSERT and protein kinase inhibition as macromolecular targets. First, all of the products

were screened through molecular docking and molecules with the highest binding free energies were further considered for molecular dynamics simulations (see Table S4). hSERT inhibition by small molecules can be useful as antidepressants. Gouaux and co-workers reported the ts3-sertraline (PDB: 6AWO) interaction.⁶⁹ The binding site and binding energy of 10j with 6AWO are similar to those of sertraline, as presented in Figure 3A. At the same time, targeting the treatment of diseases like cancer and inflammation, Sun et al.⁷⁰ reported kinase inhibition with the 8-amino-substituted 2-phenyl-2,7-naphthyridin-1(2H)-one derivative. Compound 10r is an equally good kinase inhibitor as it binds in the active sites VEGFR-2 (PDB: 3EFL), and the binding energy is very close to the reported values.

The docking results were encouraging; however, they provide static information, and their corresponding dynamics, including the perturbation of solvent environment, were thus studied using MD simulations. MD simulations are versatile tools used for determining the dynamic behavior of 10j and 10r with 6AWO and 3EFL, respectively. The preliminary analysis of the calculated trajectories was based on their root-mean-square deviation (RMSD) profile, as shown in Figure S23. The dynamics of molecule 10j with the protein (6AWO) were converged after a 40 ns time scale. However, the RMSD

was converged in ~ 150 ns for the system containing molecule **10r** complexed with 3EFL. Nevertheless, these deviations are within the range of 2 Å, which signifies the absence of any significant structural perturbations. On the other hand, the RMSD for ligand molecules in both systems was stable throughout the simulations. This is indicative of the RMSD plot for ligands that ranges within a deviation scale of 0.3 Å. Further analysis was carried out from the last 50 ns time scale of trajectories, as they achieved convergence. Here, the focus was central to the interaction between the molecules and the amino acid present in the active binding site. The key driving forces that stabilized these molecules are the hydrophobic contacts. Figure 3A shows the structural snapshot obtained from MD simulation for molecule **10j** embedded in protein. The side chains of I266, L443, and I172 were involved in stabilizing the binding via hydrophobic contacts.

Additionally, aromatic amino acids such as Y95, Y176, and F341 were involved in C–H $\cdots\pi$ interaction. The only H-bond interaction found in the putative binding site of molecule **10j** was mediated by S439. In the case of **10r**-3EFL, hydrophobic residues such as I892, L889, V899, and V916 stabilize the ligand binding within the active binding site. Aromatic amino acids such as F918 and F1047, on the other hand, were involved in edge-to-face π -stacking (Figure 3D). In addition, the charged residues K868 and D1046 were also found in the close vicinity of **10r**. The electrostatic potential maps for **10j**-6AWO and **10r**-3EFL, as shown in Figure 3B,E, respectively, further manifest that the drug molecules **10j** and **10r** reside in the hydrophobic parts of the proteins. The free energy of these molecules complexed with the protein was obtained through the MM-PBSA method. The calculated binding free energy components are shown in Table S5. Deconvolution of the free energy provides a quantitative estimate of van der Waals energy as -34.7 and -36.7 kcal mol $^{-1}$ versus the electrostatic energy, -9.4 and -2.4 kcal mol $^{-1}$, for the system containing **10j** and **10r**, respectively. This agrees with the structural analysis in a way that van der Waals forces are significantly higher due to hydrophobic contacts compared to the electrostatic interactions. Nevertheless, the free energies of solvation for the complexes in both systems were energetically equivalent. This is indicative of the ΔG_{PB} values -42.7 and -42.6 kcal mol $^{-1}$. To calculate the binding energy more precisely, the normal mode analysis was carried, thereby accounting for translational, rotational, and vibrational entropies. The relatively entropic contribution was higher in the case of **10r**. Overall, the calculated free energy indicates that both molecules are comparatively stable in their respective system. The secondary structural contents of the proteins in the presence of **10j** and **10r** were analyzed from the MD simulation and shown in Figure 3C,F. No significant changes in the secondary structures of the proteins due to the presence of **10j** and **10r** were found. In a nutshell, the docking and simulation results suggest that both the molecules are stable within the protein active sites, indicating binding energies. In addition, the protein secondary structure remains unperturbed, which is quite encouraging to consider **10j** and **10r** as promising drug candidates for hSERT and kinase inhibition, respectively.

CONCLUSIONS

In summary, we demonstrated a one-pot Friedlander condensation reaction in water using a metal-free ionic liquid (choline hydroxide) catalyst. Our methodology provides a

greener synthetic route based on mild reaction conditions to synthesize substituted 1,8-naphthyridines from 2-aminonicotinaldehyde with excellent yield. This operationally simple process was checked for diverse substrate scopes ranging from aliphatic to aromatic active methylene carbonyls. The key feature of this method is that both catalysts and products can be easily separated from the reaction mixture without further chromatographic separation. We also demonstrated that our synthesis is scalable and capable of producing multigram quantities of the products with excellent yield. DFT calculations and NCI plot index analysis suggested H-bonds between the catalyst and transition states/intermediates that facilitate the formation of the products. Choline hydroxide was found to be acting as a H-bond donor during various steps of the reaction. This property of ChOH can be exploited to design many such H-bond-assisted reactions in the future. Additionally, the products through molecular docking and MD simulations studies were found to be potential preclinical drug candidates for hSERT and kinase inhibition. We hope this inexpensive and greener synthesis approach will be adopted by many researchers while keeping in mind that the role of H-bonds with the catalysts is extremely crucial.

EXPERIMENTAL SECTION

Materials and Equipment. Commercially available compounds were purchased from different suppliers such as Sigma-Aldrich, TCI, Avra, and Spectrochem. The catalyst ChOH-IL was purchased from Sigma-Aldrich, and all of the chemicals were used without further purification unless otherwise noted. All reactions were carried out using conventional glassware at 50 °C under a N₂ atmosphere, and the reaction was monitored by TLC (thin-layer chromatography). The TLC plates (Merck TLC silica gel 60 F254) were detected under UV light ($\lambda = 254$ and 354 nm). Nuclear magnetic resonance spectra were recorded on Bruker AV 400 MHz and Jeol ECZR-400 MHz spectrometers (400 for ¹H NMR, 100 MHz for ¹³C NMR). The chemical shift values were reported relative to central CDCl₃ resonance at $\delta = 7.26$ ppm for ¹H NMR and $\delta = 77$ ppm for ¹³C NMR. High-resolution mass spectra (HRMS) were measured on a Bruker micro TOF-Q II spectrometer. The IR spectra were recorded in an FT-IR spectrometer using KBr pellets. The details of density functional theory (DFT), molecular docking, and molecular dynamics (MD) simulations are provided in the Supporting Information (SI).

General Procedure. The mixture of 2-aminonicotinaldehyde (**8**) (0.5 mmol) and carbonyl derivatives (**9–9 u**) (1.5 mmol for **9** and 0.5 mmol for the remaining carbonyls) stirred in H₂O (1 mL) followed by the addition of ChOH (1 mol %). The reaction mixture was stirred under N₂ conditions at 50 °C temperature. The completion of all of the reactions was monitored by TLC using 10% methanol/dichloromethane as the eluent. The reaction mixture was extracted from ethyl acetate (40 mL) and water (10 mL) and concentrated under vacuum. After workup, the catalyst was separated and the products were obtained with a desirable yield.

Experimental Characterization Data. *2-Methyl-1,8-naphthyridine (10)*. A mixture of 2-aminonicotinaldehyde (**8**) (61.6 mg, 0.5 mmol) and acetone (**9**) (111 μ L, 1.5 mmol) was stirred in H₂O (1 mL) followed by the addition of ChOH (3 μ L, 1 mol %). The reaction mixture was stirred under N₂ at 50 °C for 6 h. After workup, the catalyst was separated and the desired product 2-methyl-1,8-naphthyridine (**10**) was obtained

as a cream solid (71 mg, 99%). ^1H NMR (400 MHz, CDCl_3) δ 9.04 (dd, $J = 4.0, 2.0$ Hz, 1H), 8.11 (dd, $J = 2.0, 2.0$ Hz, 1H), 8.04 (d, $J = 8.4$ Hz, 1H), 7.40 (dd, $J = 4.4, 4.0$ Hz, 1H), 7.35 (d, $J = 8.0$ Hz, 1H), 2.80 (s, 3H); ^{13}C NMR (100 MHz, CDCl_3) δ 163.0, 155.9, 153.3, 136.8, 136.6, 123.0, 121.3, 120.7, 25.6.

7-Methyl-6,7,8,9-tetrahydropyrido[2,3-*b*][1,6]-naphthyridine (10i). A mixture of 2-aminonicotinaldehyde (8) (61.6 mg, 0.5 mmol) and 1-methylpiperidin-4-one (9i) (62 μL , 0.5 mmol) was stirred in H_2O (1 mL) followed by the addition of CH_3OH (3 μL , 1 mol %). The reaction mixture was stirred under N_2 at 50 °C temperature for 11 h, and the reaction progress was monitored through TLC. After completion of the reaction, the desired product 10i was separated by workup as a brown solid (92 mg, 92%). $R_f = 0.55$ (10% methanol/dichloromethane). ^1H NMR (400 MHz, CDCl_3) δ 9.01 (d, $J = 4.0$ Hz, 1H), 8.07 (d, $J = 8.0$ Hz, 1H), 7.79 (s, 1H), 7.38 (dd, $J = 4.0, 4.0$ Hz, 1H), 3.78 (s, 2H), 3.33 (t, $J = 8.0$ Hz, 2H), 2.86 (t, $J = 8.0$ Hz, 2H), 2.52 (s, 3H); ^{13}C NMR (100 MHz, CDCl_3) δ 160.0, 155.0, 153.0, 136.3, 133.4, 129.7, 121.4, 121.1, 57.4, 52.9, 46.0, 33.5; HRMS (ESI) m/z : $[\text{M} + \text{Na}]^+$ calcd for $\text{C}_{12}\text{H}_{13}\text{N}_3\text{Na}$, 222.1002; found 222.1019. mp = 115 °C. IR (KBr thin film, cm^{-1}) ν 2956, 2910, 2845, 2789, 1610, 1552, 1480, 1125, 900, 796. UV-vis λ_{abs} (max) 320 nm.

7-Ethyl-6,7,8,9-tetrahydropyrido[2,3-*b*][1,6]naphthyridine (10j). A mixture of 2-aminonicotinaldehyde (8) (61.6 mg, 0.5 mmol) and 1-ethylpiperidin-4-one (9j) (68 μL , 0.5 mmol) was stirred in H_2O (1 mL) followed by the addition of CH_3OH (3 μL , 1 mol %). The reaction mixture was stirred under N_2 at 50 °C for 10 h, and the reaction was monitored through TLC. After completion of reaction, the desired product 10j was separated by workup as a red solid (102 mg, 96%). $R_f = 0.42$ (10% methanol/dichloromethane). ^1H NMR (400 MHz, CDCl_3) δ 9.0 (dd, $J = 2.0, 2.0$ Hz, 1H), 8.05 (d, $J = 8.0$ Hz, 1H), 7.79 (s, 1H), 7.36 (dd, $J = 4.0, 4.0$ Hz, 1H), 3.82 (s, 2H), 3.31 (t, $J = 8.0$ Hz, 2H), 2.89 (t, $J = 8.0$ Hz, 2H), 2.61 (m, 2H), 1.19 (t, $J = 8.0$ Hz, 3H); ^{13}C NMR (100 MHz, CDCl_3) δ 160.5, 155.0, 152.9, 136.3, 133.6, 129.8, 121.4, 121.1, 55.1, 52.0, 50.4, 33.5, 12.3; HRMS (ESI) m/z : $[\text{M} + \text{Na}]^+$ calcd for $\text{C}_{13}\text{H}_{15}\text{N}_3\text{Na}$, 236.1158; found 236.1176. mp = 110 °C. IR (KBr thin film, cm^{-1}) ν 2972, 2938, 2816, 2766, 1620, 1560, 1483, 1140, 910, 792. UV-vis λ_{abs} (max) 320 nm.

■ ASSOCIATED CONTENT

SI Supporting Information

The Supporting Information is available free of charge at <https://pubs.acs.org/doi/10.1021/acsomega.1c02798>.

^1H and ^{13}C NMR spectra, computational methods for DFT, optimized cartesian coordinates, ADMET properties, and classical simulations (PDF)

■ AUTHOR INFORMATION

Corresponding Author

Himansu S. Biswal – School of Chemical Sciences, National Institute of Science Education and Research (NISER), 752050 Bhubaneswar, India; Homi Bhabha National Institute, Mumbai 400094, India; orcid.org/0000-0003-0791-2259; Phone: +91-674-2494 185; Email: himansu@niser.ac.in

Authors

Shubhranshu Shekhar Choudhury – School of Chemical Sciences, National Institute of Science Education and Research (NISER), 752050 Bhubaneswar, India; Homi Bhabha National Institute, Mumbai 400094, India

Subhrakant Jena – School of Chemical Sciences, National Institute of Science Education and Research (NISER), 752050 Bhubaneswar, India; Homi Bhabha National Institute, Mumbai 400094, India; orcid.org/0000-0001-9474-821X

Dipak Kumar Sahoo – School of Chemical Sciences, National Institute of Science Education and Research (NISER), 752050 Bhubaneswar, India; Homi Bhabha National Institute, Mumbai 400094, India; orcid.org/0000-0002-6900-3897

Shamasoddin Shekh – Department of Chemistry, Central University of Karnataka, Kalaburagi 585367 Karnataka, India

Rajiv K. Kar – Fritz Haber Center for Molecular Dynamics, Institute of Chemistry, The Hebrew University of Jerusalem, Jerusalem 9190401, Israel; orcid.org/0000-0003-4629-5863

Ambuj Dhakad – School of Chemical Sciences, National Institute of Science Education and Research (NISER), 752050 Bhubaneswar, India; Homi Bhabha National Institute, Mumbai 400094, India

Konkallu Hanumae Gowd – Department of Chemistry, Central University of Karnataka, Kalaburagi 585367 Karnataka, India; orcid.org/0000-0002-8991-9368

Complete contact information is available at:

<https://pubs.acs.org/doi/10.1021/acsomega.1c02798>

Author Contributions

H.S.B. designed the project. S.S.C. and S.J. carried out synthesis and characterization. S.S.C., S.J., A.D., and H.S.B. performed DFT calculations. Molecular docking studies were done by S.S.C., S.S., S.J., and K.H.G. R.K.K. performed the MD analysis. The manuscript was written through the contributions of all authors. All authors have approved the final version of the manuscript.

Funding

S.S.C., S.J., D.K., A.D., and H.S.B. acknowledge financial support from the Department of Atomic Energy, Science and Engineering Research Board (SERB), Department of Science and Technology (DST) (Project File No: CRG/2018/000892), Govt. of India.

Notes

The authors declare no competing financial interest.

■ ACKNOWLEDGMENTS

This manuscript is dedicated to the 80th birthday of Prof. Anadi Charan Dash and the 65th birthday of Prof. Sanjay Wategaonkar. S.S.C., S.J., D.K., A.D., and H.S.B. acknowledge the Centre for Interdisciplinary Sciences (CIS), NISER, for the experimental facilities.

■ REFERENCES

- (1) Bisacchi, G. S. Origins of the Quinolone Class of Antibacterials: An Expanded "Discovery Story". *J. Med. Chem.* **2015**, *58*, 4874–4882.
- (2) Bao, J.; Marathe, B.; Govorkova, E. A.; Zheng, J. J. Drug Repurposing Identifies Inhibitors of Oseltamivir-Resistant Influenza Viruses. *Angew. Chem., Int. Ed.* **2016**, *55*, 3438–3441.

- (3) Ahmed, M.; Kelley, S. O. Enhancing the Potency of Nalidixic Acid toward a Bacterial DNA Gyrase with Conjugated Peptides. *ACS Chem. Biol.* **2017**, *12*, 2563–2569.
- (4) Pham, T. D. M.; Ziora, Z. M.; Blaskovich, M. A. T. Quinolone antibiotics. *Med. Chem. Comm* **2019**, *10*, 1719–1739.
- (5) Zhao, X. Z.; Smith, S. J.; Métifiot, M.; Marchand, C.; Boyer, P. L.; Pommier, Y.; Hughes, S. H.; Burke, T. R. 4-Amino-1-hydroxy-2-oxo-1,8-naphthyridine-Containing Compounds Having High Potency against Raltegravir-Resistant Integrase Mutants of HIV-1. *J. Med. Chem.* **2014**, *57*, S190–S202.
- (6) Chen, T. C.; Hsu, Y. L.; Tsai, Y. C.; Chang, Y. W.; Kuo, P. L.; Chen, Y. H. Gemifloxacin inhibits migration and invasion and induces mesenchymal-epithelial transition in human breast adenocarcinoma cells. *J. Mol. Med.* **2014**, *92*, 53–64.
- (7) Taha, M. O.; Bustanji, Y.; Al-Ghusein, M. A. S.; Mohammad, M.; Zalloum, H.; Al-Masri, I. M.; Atallah, N. Pharmacophore Modeling, Quantitative Structure–Activity Relationship Analysis, and in Silico Screening Reveal Potent Glycogen Synthase Kinase-3 β Inhibitory Activities for Cimetidine, Hydroxychloroquine, and Gemifloxacin. *J. Med. Chem.* **2008**, *51*, 2062–2077.
- (8) Strickland, S. A.; Podoltsev, N. A.; Mohan, S. R.; Zeidan, A. M.; Childress, M. A.; Ayers, G. D.; Byrne, M. T.; Gore, S. D.; Stuart, R. K.; Savona, M. R. The VITAL Trial: Phase II Trial of Vosaroxin and Infusional Cytarabine for Frontline Treatment of acute Myeloid Leukemia. *Blood* **2019**, *134*, 180.
- (9) Ravandi, F.; Ritchie, E. K.; Sayar, H.; Lancet, J. E.; Craig, M.; Vey, N.; Strickland, S. A.; Schiller, G. J.; Jabbour, E. J.; Erba, H. P.; Pignaux, A.; Horst, H.-A.; Recher, C.; Klimek, V. M.; Cortes, J. E.; Roboz, G. J.; Craig, A. R.; Ward, R.; Smith, J.; Kantarjian, H. M.; Stuart, R. K. Durable Overall Survival Benefit in Patients \geq 60 Years with Relapsed or Refractory AML Treated with Vosaroxin/Cytarabine Vs Placebo/Cytarabine: Updated Results from the Valor Trial. *Blood* **2016**, *128*, 903.
- (10) Sasine, J. P.; Schiller, G. J. Emerging strategies for high-risk and relapsed/refractory acute myeloid leukemia: Novel agents and approaches currently in clinical trials. *Blood Rev.* **2015**, *29*, 1–9.
- (11) Griswold, A.; Bloom, S.; Lectka, T. A Chelating Nucleophile Plays a Starring Role: 1,8-Naphthyridine-Catalyzed Polycomponent α,α -Difluorination of Acid Chlorides. *J. Org. Chem.* **2014**, *79*, 9830–9834.
- (12) Oyama, D.; Abe, R.; Takase, T. Coordination chemistry of mononuclear ruthenium complexes bearing versatile 1,8-naphthyridine units: Utilization of specific reaction sites constructed by the secondary coordination sphere. *Coord. Chem. Rev.* **2018**, *375*, 424–433.
- (13) Huang, X.-C.; Xu, R.; Chen, Y.-Z.; Zhang, Y.-Q.; Shao, D. Two Four-Coordinate and Seven-Coordinate CoII Complexes Based on the Bidentate Ligand 1, 8-Naphthyridine Showing Slow Magnetic Relaxation Behavior. *Chem. Asian J.* **2020**, *15*, 279–286.
- (14) He, C.; Barrios, A. M.; Lee, D.; Kuzelka, J.; Davydov, R. M.; Lippard, S. J. Diiron Complexes of 1,8-Naphthyridine-Based Dinucleating Ligands as Models for Hemerythrin. *J. Am. Chem. Soc.* **2000**, *122*, 12683–12690.
- (15) Margiotta, N.; Savino, S.; Gandin, V.; Marzano, C.; Natile, G. Monofunctional Platinum(II) Complexes with Potent Tumor Cell Growth Inhibitory Activity: The Effect of a Hydrogen-Bond Donor/Acceptor N-Heterocyclic Ligand. *ChemMedChem* **2014**, *9*, 1161–1168.
- (16) Shen, Y.-F.; Zhao, W.-L.; Lu, H.-Y.; Wang, Y.-F.; Zhang, D.-W.; Li, M.; Chen, C.-F. Naphthyridine-based thermally activated delayed fluorescence emitters for highly efficient blue OLEDs. *Dyes Pigm.* **2020**, *178*, No. 108324.
- (17) Silvestri, I.; Lyu, H.; Fata, F.; Boumis, G.; Miele, A. E.; Ardini, M.; Ippoliti, R.; Bellelli, A.; Jadhav, A.; Lea, W. A.; Simeonov, A.; Cheng, Q.; Arnér, E. S. J.; Thatcher, G. R. J.; Petukhov, P. A.; Williams, D. L.; Angelucci, F. Fragment-Based Discovery of a Regulatory Site in Thioredoxin Glutathione Reductase Acting as “Doorstop” for NADPH Entry. *ACS Chem. Biol.* **2018**, *13*, 2190–2202.
- (18) Wood, D. J.; Lopez-Fernandez, J. D.; Knight, L. E.; Al-Khawaldeh, I.; Gai, C.; Lin, S.; Martin, M. P.; Miller, D. C.; Cano, C.; Endicott, J. A.; Hardcastle, I. R.; Noble, M. E. M.; Waring, M. J. FragLites—Minimal, Halogenated Fragments Displaying Pharmacophore Doublets. An Efficient Approach to Druggability Assessment and Hit Generation. *J. Med. Chem.* **2019**, *62*, 3741–3752.
- (19) Friedlaender, P. Ueber o-Amidobenzaldehyd. *Ber. Dtsch. Chem. Ges.* **1882**, *15*, 2572–2575.
- (20) Koller, G. Über eine Synthese von Derivaten des 1,8-Naphthyridins. *Ber. Dtsch. Chem. Ges. (A and B Series)* **1927**, *60*, 407–410.
- (21) Panday, A. K.; Mishra, R.; Jana, A.; Parvin, T.; Choudhury, L. H. Synthesis of Pyrimidine Fused Quinolines by Ligand-Free Copper-Catalyzed Domino Reactions. *J. Org. Chem.* **2018**, *83*, 3624–3632.
- (22) Chaudhari, C.; Sato, K.; Ogura, Y.; Miayahara, S.-I.; Nagaoka, K. Pr2O3 Supported Nano-layered Ruthenium Catalyzed Acceptorless Dehydrogenative Synthesis of 2-Substituted Quinolines and 1,8-Naphthyridines from 2-Aminoaryl Alcohols and Ketones. *ChemCatChem* **2020**, *12*, 2198–2202.
- (23) Das, A.; Anbu, N.; Varalakshmi, P.; Dhakshinamoorthy, A.; Biswas, S. A hydrazine functionalized UiO-66(Hf) metal–organic framework for the synthesis of quinolines via Friedländer condensation. *New J. Chem.* **2020**, *44*, 10982–10988.
- (24) Senadi, G. C.; Dhandabani, G. K.; Hu, W.-P.; Wang, J.-J. Metal-free annulation/aerobic oxidative dehydrogenation of cyclohexanones with o-acylanilines: efficient syntheses of acridines. *Green Chem.* **2016**, *18*, 6241–6245.
- (25) Marco-Contelles, J.; Pérez-Mayoral, E.; Samadi, A.; Carreiras, M. dC.; Soriano, E. Recent Advances in the Friedländer Reaction. *Chem. Rev.* **2009**, *109*, 2652–2671.
- (26) Lipshutz, B. H.; Ghorai, S.; Cortes-Clerget, M. The Hydrophobic Effect Applied to Organic Synthesis: Recent Synthetic Chemistry “in Water”. *Chem.–Eur. J.* **2018**, *24*, 6672–6695.
- (27) Tarczykowska, A. Green solvents. *J. Phys. Educ.* **2017**, *7*, 224–232.
- (28) Batista, V. F.; Pinto, D. C. G. A.; Silva, A. M. S. Synthesis of Quinolines: A Green Perspective. *ACS Sustainable Chem. Eng.* **2016**, *4*, 4064–4078.
- (29) Campos, J. F.; Berteina-Raboin, S. Greener Synthesis of Nitrogen-Containing Heterocycles in Water, PEG, and Bio-Based Solvents. *Catalysts* **2020**, *10*, No. 429.
- (30) Anderson, E. C.; Sneddon, H. F.; Hayes, C. J. A mild synthesis of substituted 1,8-naphthyridines. *Green Chem.* **2019**, *21*, 3050–3058.
- (31) Rezayati, S.; Jafroudi, M. T.; Nezhad, E. R.; Hajinasiri, R.; Abbaspour, S. Imidazole-functionalized magnetic Fe3O4 nanoparticles: an efficient, green, recyclable catalyst for one-pot Friedländer quinoline synthesis. *Res. Chem. Intermed.* **2016**, *42*, 5887–5898.
- (32) Chen, C.; Chen, C.; Li, B.; Tao, J.; Peng, J. Aqueous Synthesis of 1-H-2-Substituted Benzimidazoles via Transition-Metal-Free Intramolecular Amination of Aryl Iodides. *Molecules* **2012**, *17*, 12506–12520.
- (33) Xie, L.-Y.; Duan, Y.; Lu, L.-H.; Li, Y.-J.; Peng, S.; Wu, C.; Liu, K.-J.; Wang, Z.; He, W.-M. Fast, Base-Free and Aqueous Synthesis of Quinolin-2(1H)-ones under Ambient Conditions. *ACS Sustainable Chem. Eng.* **2017**, *5*, 10407–10412.
- (34) Chapman, M. R.; Kwan, M. H. T.; King, G. E.; Kyffin, B. A.; Blacker, A. J.; Willans, C. E.; Nguyen, B. N. Rapid, metal-free and aqueous synthesis of imidazo[1,2-a]pyridine under ambient conditions. *Green Chem.* **2016**, *18*, 4623–4627.
- (35) Prat, D.; Wells, A.; Hayler, J.; Sneddon, H.; McElroy, C. R.; Abou-Shehada, S.; Dunn, P. J. CHEM21 selection guide of classical and less classical-solvents. *Green Chem.* **2016**, *18*, 288–296.
- (36) Narayan, S.; Muldoon, J.; Finn, M. G.; Fokin, V. V.; Kolb, H. C.; Sharpless, K. B. “On Water”: Unique Reactivity of Organic Compounds in Aqueous Suspension. *Angew. Chem., Int. Ed.* **2005**, *44*, 3275–3279.
- (37) Sheldon, R. Catalytic reactions in ionic liquids. *Chem. Commun.* **2001**, *23*, 2399–2407.

- (38) Madeira Lau, R.; Van Rantwijk, F.; Seddon, K. R.; Sheldon, R. A. Lipase-Catalyzed Reactions in Ionic Liquids. *Org. Lett.* **2000**, *2*, 4189–4191.
- (39) Sheldon, R. A.; Lau, R. M.; Sorgedraeger, M. J.; van Rantwijk, F.; Seddon, K. R. Biocatalysis in ionic liquids. *Green Chem.* **2002**, *4*, 147–151.
- (40) Pant, P. L.; Sonune, R. K.; Shankarling, G. S. Choline Hydroxide Promoted Synthesis of N-Aryl Anthraquinone Derivatives: Metal Free Approach to Ullmann Coupling Reactions. *ChemistrySelect* **2018**, *3*, 5249–5253.
- (41) Abelló, S.; Medina, F.; Rodríguez, X.; Cesteros, Y.; Salagre, P.; Sueiras, J. E.; Tichit, D.; Coq, B. Supported choline hydroxide (ionic liquid) as heterogeneous catalyst for aldol condensation reactions. *Chem. Commun.* **2004**, *9*, 1096–1097.
- (42) Sahoo, D. K.; Jena, S.; Dutta, J.; Chakrabarty, S.; Biswal, H. S. Critical Assessment of the Interaction between DNA and Choline Amino Acid Ionic Liquids: Evidences of Multimodal Binding and Stability Enhancement. *ACS Cent. Sci.* **2018**, *4*, 1642–1651.
- (43) Sahoo, D. K.; Jena, S.; Tulsian, K. D.; Dutta, J.; Chakrabarty, S.; Biswal, H. S. Amino-Acid-Based Ionic Liquids for the Improvement in Stability and Activity of Cytochrome c: A Combined Experimental and Molecular Dynamics Study. *J. Phys. Chem. B* **2019**, *123*, 10100–10109.
- (44) Sahoo, D. K.; Chand, A.; Jena, S.; Biswal, H. S. Hydrogen-bond-driven thioracil dissolution in aqueous ionic liquid: A combined microscopic, spectroscopic and molecular dynamics study. *J. Mol. Liq.* **2020**, *319*, No. 114275.
- (45) Jokić, M.; Raza, Z.; Katalenić, D. The Synthesis of Novel 6,5- and 6,6-Membered Fused Heterocyclic Compounds Derived from Thymine. *Nucleosides, Nucleotides Nucleic Acids* **2000**, *19*, 1381–1396.
- (46) Guajardo, J.; Ibanez, A.; Guerschais, V.; Vega, A.; Moya, S.; Aguirre, P. Ruthenium(II)-carbonyl complexes containing two N-monodentate 1,8-naphthyridine ligands: active catalysis in transfer hydrogenation reactions. *Acta Crystallogr., Sect. C: Struct. Chem.* **2018**, *74*, 1547–1552.
- (47) Das, A.; Jana, A.; Maji, B. Palladium-catalyzed remote C–H functionalization of 2-aminopyrimidines. *Chem. Commun.* **2020**, *56*, 4284–4287.
- (48) Dutta, U.; Maiti, S.; Pimparkar, S.; Maiti, S.; Gahan, L. R.; Krenske, E. H.; Lupton, D. W.; Maiti, D. Rhodium catalyzed template-assisted distal para-C–H olefination. *Chem. Sci.* **2019**, *10*, 7426–7432.
- (49) de los Ríos, C.; Marco-Contelles, J. Tacrines for Alzheimer's disease therapy. III. The PyridoTacrines. *Eur. J. Med. Chem.* **2019**, *166*, 381–389.
- (50) Li, X.; Wang, H.; Xu, Y.; Liu, W.; Gong, Q.; Wang, W.; Qiu, X.; Zhu, J.; Mao, F.; Zhang, H.; Li, J. Novel Vilazodone–Tacrines Hybrids as Potential Multitarget-Directed Ligands for the Treatment of Alzheimer's Disease Accompanied with Depression: Design, Synthesis, and Biological Evaluation. *ACS Chem. Neurosci.* **2017**, *8*, 2708–2721.
- (51) Acosta, P.; Butassi, E.; Insuasty, B.; Ortiz, A.; Abonia, R.; Zacchino, S. A.; Quiroga, J. Microwave-Assisted Synthesis of Novel Pyrazolo[3,4-g][1,8]naphthyridin-5-amine with Potential Antifungal and Antitumor Activity. *Molecules* **2015**, *20*, 8499–8520.
- (52) de los Ríos, C.; Egea, J.; Marco-Contelles, J.; León, R.; Samadi, A.; Iriepa, I.; Moraleda, I.; Gálvez, E.; García, A. G.; López, M. G.; Villarroja, M.; Romero, A. Synthesis, Inhibitory Activity of Cholinesterases, and Neuroprotective Profile of Novel 1,8-Naphthyridine Derivatives. *J. Med. Chem.* **2010**, *53*, 5129–5143.
- (53) Taylor, M. S.; Jacobsen, E. N. Asymmetric Catalysis by Chiral Hydrogen-Bond Donors. *Angew. Chem., Int. Ed.* **2006**, *45*, 1520–1543.
- (54) Schreiner, P. R.; Wittkopp, A. H-Bonding Additives Act Like Lewis Acid Catalysts. *Org. Lett.* **2002**, *4*, 217–220.
- (55) Wittkopp, A.; Schreiner, P. R. Metal-Free, Noncovalent Catalysis of Diels–Alder Reactions by Neutral Hydrogen Bond Donors in Organic Solvents and in Water. *Chem.-Eur. J.* **2003**, *9*, 407–414.
- (56) Dethlefs, C.; Eckelmann, J.; Kobarg, H.; Weyrich, T.; Brammer, S.; Näther, C.; Lüning, U. Determination of Binding Constants of Hydrogen-Bonded Complexes by ITC, NMR CIS, and NMR Diffusion Experiments. *Eur. J. Org. Chem.* **2011**, *2011*, 2066–2074.
- (57) Johnson, E. R.; Keinan, S.; Mori-Sánchez, P.; Contreras-García, J.; Cohen, A. J.; Yang, W. Revealing Noncovalent Interactions. *J. Am. Chem. Soc.* **2010**, *132*, 6498–6506.
- (58) Contreras-García, J.; Johnson, E. R.; Keinan, S.; Chaudret, R.; Piquemal, J.-P.; Beratan, D. N.; Yang, W. NCIPLLOT: A Program for Plotting Noncovalent Interaction Regions. *J. Chem. Theory Comput.* **2011**, *7*, 625–632.
- (59) Mundlapati, V. R.; Sahoo, D. K.; Bhaumik, S.; Jena, S.; Chandrakar, A.; Biswal, H. S. Noncovalent Carbon-Bonding Interactions in Proteins. *Angew. Chem., Int. Ed.* **2018**, *57*, 16496–16500.
- (60) Sahoo, D. K.; Jena, S.; Dutta, J.; Rana, A.; Biswal, H. S. Nature and Strength of M–H···S and M–H···Se (M = Mn, Fe, & Co) Hydrogen Bond. *J. Phys. Chem. A* **2019**, *123*, 2227–2236.
- (61) Chand, A.; Sahoo, D. K.; Rana, A.; Jena, S.; Biswal, H. S. The Prodigious Hydrogen Bonds with Sulfur and Selenium in Molecular Assemblies, Structural Biology, and Functional Materials. *Acc. Chem. Res.* **2020**, *53*, 1580–1592.
- (62) Abdullayev, Y.; Abbasov, V.; Ducati, L. C.; Talybov, A.; Autschbach, J. Ionic Liquid Solvation versus Catalysis: Computational Insight from a Multisubstituted Imidazole Synthesis in [Et2NH2][HSO4]. *ChemistryOpen* **2016**, *5*, 460–469.
- (63) Butina, D.; Segall, M. D.; Frankcombe, K. Predicting ADME properties in silico: methods and models. *Drug Discovery Today* **2002**, *7*, S83–S88.
- (64) van de Waterbeemd, H.; Gifford, E. ADMET in silico modelling: towards prediction paradise? *Nat. Rev. Drug. Discov.* **2003**, *2*, 192–204.
- (65) Barraza, S. J.; Denmark, S. E. Synthesis, Reactivity, Functionalization, and ADMET Properties of Silicon-Containing Nitrogen Heterocycles. *J. Am. Chem. Soc.* **2018**, *140*, 6668–6684.
- (66) Zhu, Y.; Han, Y.; Ma, Y.; Yang, P. ADME/toxicity prediction and antitumor activity of novel nitrogenous heterocyclic compounds designed by computer targeting of alkylglycerone phosphate synthase. *Oncol. Lett.* **2018**, *16*, 1431–1438.
- (67) Lipinski, C. A.; Lombardo, F.; Dominy, B. W.; Feeney, P. J. Experimental and computational approaches to estimate solubility and permeability in drug discovery and development settings. *Adv. Drug Del. Rev.* **2012**, *64*, 4–17.
- (68) Jorgensen, W. L.; Duffy, E. M. Prediction of drug solubility from Monte Carlo simulations. *Bioorg. Med. Chem. Lett.* **2000**, *10*, 1155–8.
- (69) Coleman, J. A.; Gouaux, E. Structural basis for recognition of diverse antidepressants by the human serotonin transporter. *Nat. Struct. Mol. Biol.* **2018**, *25*, 170–175.
- (70) Sun, H.; Zhuo, L.; Dong, H.; Huang, W.; She, N. Discovery of 8-Amino-Substituted 2-Phenyl-2,7-Naphthyridinone Derivatives as New c-Kit/VEGFR-2 Kinase Inhibitors. *Molecules* **2019**, *24*, No. 4461.